

# Triphenylamine Derived Radical Cations for Colorimetric Cu<sup>2+</sup> Sensors and as an Antibacterial Agent

Luqi He<sup>[a]</sup>, Jiao Tan<sup>[b]</sup>, Chun Liu<sup>[a]</sup>, Shouting Wu<sup>[c]</sup>, Qi-Long Zhang<sup>[c]</sup>, Carl Redshaw<sup>[d]\*</sup> and Xin-Long Ni<sup>\*[a,b]</sup>

[a] L. He, C. Liu, Prof. X.-L. Ni

Key Laboratory of Macrocyclic and Supramolecular Chemistry of Guizhou Province, Guizhou University, Guiyang 550025, China.

E-mail: [longni333@163.com](mailto:longni333@163.com)

[b] J. Tan, Prof. X.-L. Ni

Key Laboratory of the Assembly and Application of Organic Functional Molecules of Hunan Province, Hunan Normal University, Changsha 410081, China

[c] S. Wu, Prof. Q. Zhang

School of Basic Medical Science/School of Public Health, Guizhou Medical University, Guiyang, 550025, China

[d] Prof. C. Redshaw

Department of Chemistry, University of Hull, Hull HU6 7RX, UK

E-mail: [C.Redshaw@hull.ac.uk](mailto:C.Redshaw@hull.ac.uk)

Supporting information for this article is given via a link at the end of the document. ((Please delete this text if not appropriate))

**Abstract:** Herein, a series of triphenylamine derivatives (TPAs), which are comprised of electron donor and acceptor moieties, have been exploited as sensitive colorimetric sensors for Cu<sup>2+</sup>, operating via the formation of the corresponding organic radicals through a redox reaction in a mixed solvent system (acetonitrile/water). Further studies indicated that the Cu<sup>2+</sup> recognition triggered organic radical cations were stable in aqueous solution, and can be used as an antibacterial agent for both *Escherichia coli* (*E. coli*) and *Staphylococcus aureus* (*S. aureus*) at very low concentrations (10<sup>-7</sup> M). On comparison with light irradiated photodynamic therapy triggered radicals, the present work reveals that the direct use of radical cations of TPAs is more convenient for practical applications in killing bacteria. This work thus provides new insight into the design of sensitive colorimetric sensors and antibacterial agents.

## Introduction

Organic radical cations have attracted increasing attention because of their applications in catalysis, mixed-valence materials, and biomedicines.<sup>[1-3]</sup> Meanwhile, studies have indicated that free organic radicals can be exploited as probe sensors, which is attributed to their remarkable UV-vis absorption changes.<sup>[4-8]</sup> For example, Gopidas and co-workers revealed that aromatic amine radical cations could be generated with a fast response by mixing of the aromatic amines with Cu<sup>2+</sup> in acetonitrile (ACN) solution, where Cu<sup>2+</sup> can accept an electron from the aromatic amines and thereby form the corresponding amine radical cations.<sup>[9]</sup> Compared to other methods of amine radical cation generation including anodic oxidation, photoionization, and photoinduced electron transfer, where the amine radical cations are generated as transient intermediates, this approach allows for the generation of stable organic radical cations with distinct color changes in a very simple operation.<sup>[10]</sup> Thus, a series of colorimetric Cu<sup>2+</sup> sensors have been reported on the basis of generating the corresponding organic radical cations via the redox couple Cu<sup>2+</sup>/Cu<sup>+</sup> in N-containing  $\pi$ -systems.<sup>[11-14]</sup> However, the recognition of Cu<sup>2+</sup> using this approach in aqueous media is somewhat limited.

The Cu<sup>2+</sup> ion is an essential nutrient for life and plays an important role in the areas of biological, environmental,

and chemical systems.<sup>[15,16]</sup> However, either an excess or a deficiency of Cu<sup>2+</sup> ions may lead to the deterioration of vital organs and to the progression of complications such as Menkes and Wilson diseases and Alzheimer's disease.<sup>[17, 18]</sup> As a result, many methods have been developed for the trace detection of Cu<sup>2+</sup> ions in biological and environmental systems. Among these approaches, fluorescence spectroscopy is a frequently used technique because of its high sensitivity and low cost.<sup>[19-21]</sup> However, fluorescence quenching generally occurred in the detection procedure of Cu<sup>2+</sup> ion due to its intrinsic paramagnetic nature,<sup>[22]</sup> which seriously reduced the detection sensitivity of the sensors.

Alternatively, the use of colorimetric sensors is the other valuable approach for the detection of Cu<sup>2+</sup> ions,<sup>[23-26]</sup> but the lesser sensitivity of UV-vis absorption compared to fluorescence emission is the main disadvantage of this method. Therefore, the key factor in improving the sensitivity of colorimetric sensors is to enhance their molar absorption coefficient ( $\epsilon$ ). To achieve a high  $\epsilon$  in the UV-vis absorption spectra of colorimetric sensors, an effective approach is to introduce strong electron donor and acceptor groups into the  $\pi$ -conjugated chromophores. Indeed, numerous studies have suggested that the use of  $\pi$ -conjugated organic chromophores, incorporating D-A units in their backbone, affords properties such as broad light absorption in the visible range, low band gap and high electric conductivity.<sup>[27-29]</sup> Reports on organic radical cation-based colorimetric sensors that feature improved sensitivity via an appended D-A structure are scant.<sup>[30]</sup>

In this work, 4',4''-dimethoxytriphenylamine derivatives (TPAs) including TPA-Br, TPA-Py and TPA-Py<sup>+</sup> have been exploited as D-A appended colorimetric sensors. Results indicated that the highly sensitive and selective colorimetric detection of Cu<sup>2+</sup> was achieved via a redox reaction with a distinct color change in a mixed solvent of ACN and water. Further studies indicated that the Cu<sup>2+</sup> recognition triggered organic radical cations can be used as antibacterial agents and were found to exhibit highly antibacterial efficiency toward both *Escherichia coli* (*E. coli*) and *Staphylococcus aureus* (*S. aureus*)

## Results and Discussion

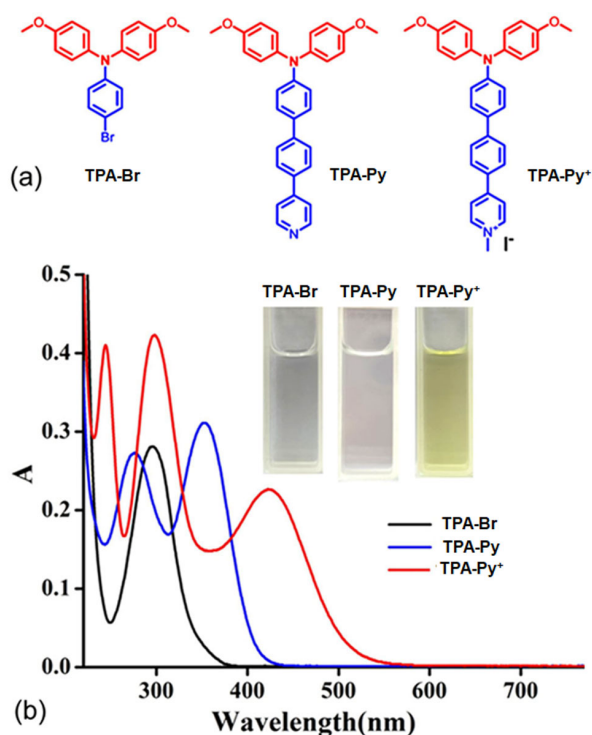


**Figure 1.** (a) Chemical structures of **TPA-Br**, **TPA-Py** and **TPA-Py<sup>+</sup>**, (b) UV-vis absorption spectra of **TPA-Br**, **TPA-Py** and **TPA-Py<sup>+</sup>** (at  $1.0 \times 10^{-5}$  M) in acetonitrile solution.

As shown in **Figure 1a**, **TPA-py** and **TPA-py<sup>+</sup>** were synthesized in high yield from **TPA-Br** by a standard Suzuki cross-coupling reaction, with methoxybenzene as the electron donor moiety. Their UV-vis absorptions were recorded in ACN solution. As can be seen from **Figure 1b**, the solutions of **TPA-Br**, **TPA-Py** and **TPA-Py<sup>+</sup>** exhibited a typical triphenylamine absorption maximum at around 295 nm, corresponding to the  $\pi$ - $\pi^*$  transition of the parent aromatic motifs, while remarkable charge transfer (CT) peaks with a red-shift at 388 nm and 432 nm for **TPA-Py** and **TPA-Py<sup>+</sup>**, respectively were observed. This indicated a strong electronic communication between the donor methoxybenzene and the acceptor pyridine core. The corresponding  $\epsilon$  values for **TPA-Br**, **TPA-Py** and **TPA-Py<sup>+</sup>** were determined to be  $2.81 \times 10^4 \text{ M}^{-1}\cdot\text{cm}^{-1}$ ,  $3.11 \times 10^4 \text{ M}^{-1}\cdot\text{cm}^{-1}$ , and  $4.23 \times 10^4 \text{ M}^{-1}\cdot\text{cm}^{-1}$ , respectively. Clearly, the bathochromic shift of the UV-vis absorption and the increased value of  $\epsilon$  for **TPA-Br** to **TPA-Py<sup>+</sup>** suggested that the strategy of D-A is an efficient approach in regulating the photophysical properties of such dye molecules.

In order to gain detailed electronic structural information on the D-A system, density functional theory (DFT) calculations were performed at the B3LYP/6-31G\* level and acetonitrile was selected as the solvent. The contours of the HOMO and LUMO of **TPA-Br**, **TPA-Py** and **TPA-Py<sup>+</sup>** are shown in **Figure 2**. The computational results imply that the HOMO orbitals of the three molecules are localized over the methoxybenzene derived triphenylamine unit, whereas the LUMO is delocalized over the bipyridine

moiety. Close inspection revealed that the energy levels of the LUMOs of **TPA-Py** and **TPA-Py<sup>+</sup>** undergo a significant decrease relative to **TPA-Br**, and no obvious changes were observed in the energy levels of the corresponding HOMO orbital. As a result, the HOMO–LUMO gap in **TPA-Br**, **TPA-Py** and **TPA-Py<sup>+</sup>** are 4.3169 eV, 3.3623 eV, 2.2096 eV, respectively. The trend observed in the HOMO–LUMO gap displays the order **TPA-Br** > **TPA-Py** > **TPA-Py<sup>+</sup>**. These results suggested that the incorporation of bipyridine and its cationic species efficiently lowers the HOMO–LUMO gap, which show good agreement with the corresponding experimental optical properties. In particular, the unchanged HOMO energies of **TPA-Py** and **TPA-Py<sup>+</sup>** indicated similar electron transfer (ET) reactions can take place upon mixing with  $\text{Cu}^{2+}$ .<sup>[10]</sup>

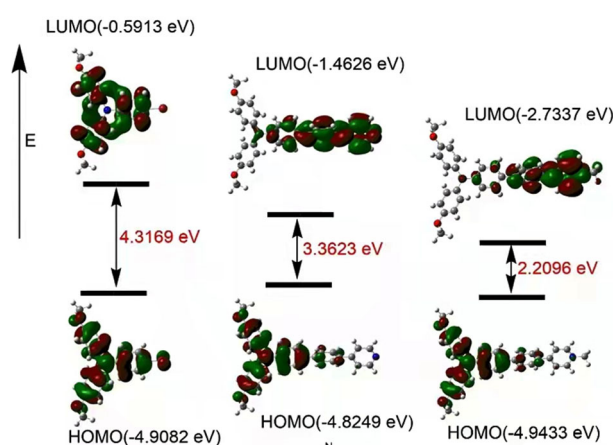


**Figure 2.** B3LYP/6-31G\*-calculated frontier HOMOs and LUMOs of **TPA-Br**, **TPA-Py** and **TPA-Py<sup>+</sup>**.

In an effort to obtain more practical conditions for the realization of the **TPA**-based organic radical selectivity for the targeting of  $\text{Cu}^{2+}$  cations, various perchlorate salts, such as  $\text{Li}^+$ ,  $\text{Na}^+$ ,  $\text{Cd}^{2+}$ ,  $\text{Al}^{3+}$ ,  $\text{Fe}^{3+}$ ,  $\text{Zn}^{2+}$ ,  $\text{K}^+$ ,  $\text{Hg}^{2+}$ ,  $\text{Ca}^{2+}$ ,  $\text{Cs}^+$ ,  $\text{Ba}^{2+}$ ,  $\text{Mg}^{2+}$ ,  $\text{Ni}^{2+}$ ,  $\text{Pb}^{2+}$ ,  $\text{Co}^{2+}$ ,  $\text{Ba}^{2+}$ ,  $\text{Ag}^+$ ,  $\text{Cu}^{2+}$  were directly added to the ACN/water solution (99:1, v:v) of **TPA-Br**, **TPA-Py** and **TPA-Py<sup>+</sup>**, respectively. As can be seen from **Figures 3a-c**, on addition of  $\text{Cu}^{2+}$ , new absorbance peaks in the visible and NIR regions at around 364, 580, and 748 nm were observed for the **TPA-Br** solution, peaks at 408, 610, and 748 nm were observed for the **TPA-Py** solution, and peaks at 371, 610, and 748 nm were observed for the **TPA-Py<sup>+</sup>** solution (the UV-vis absorption peak of pure  $\text{Cu}(\text{ClO}_4)_2$  was appeared at 980 nm, **Figure S1**). Importantly, no significant UV-vis absorption spectral changes appeared upon addition of the other tested metal cations to the solution, with the exception of **TPA-Py**, where a slightly red-shifted absorption peak was observed in the presence of  $\text{Cd}^{2+}$ ,  $\text{Al}^{3+}$ ,  $\text{Fe}^{3+}$ ,  $\text{Zn}^{2+}$ ,  $\text{Pb}^{2+}$  ions, which may be attributed to the ease of coordination of these cations to the pyridine nitrogen atom of **TPA-Py** leading to an increased intramolecular charge transfer (ICT) effect. Meanwhile, the extremely rapid and distinct color change of the sensors from colorless or pale yellow to blue or green can be observed by the naked eye in the presence of  $\text{Cu}^{2+}$  (inserts of **Figures 3a-c**).

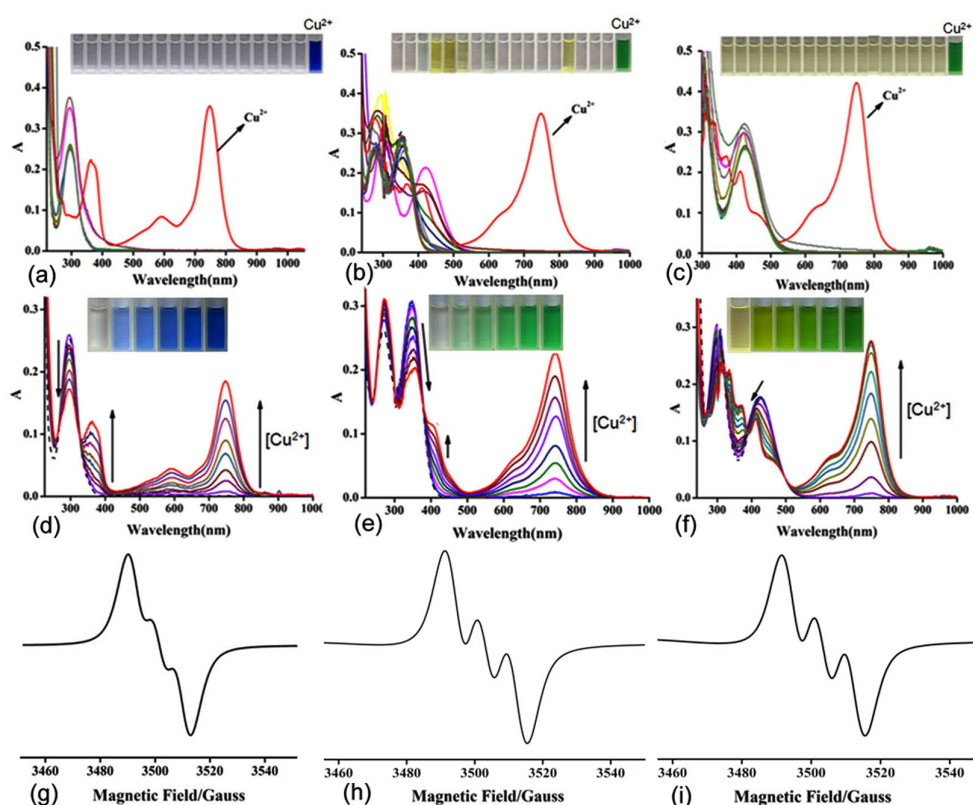


**Figure 3.** UV-vis absorption spectra of (a) **TPA-Br**, (b) **TPA-Py**, (c) **TPA-Py\*** (at  $1.0 \times 10^{-5}$  M in ACN/water solution, 99:1, v/v) in the presence of various metal ions including Li<sup>+</sup>, Na<sup>+</sup>, Cd<sup>2+</sup>, Al<sup>3+</sup>, Fe<sup>3+</sup>, Zn<sup>2+</sup>, K<sup>+</sup>, Hg<sup>2+</sup>, Ca<sup>2+</sup>, Cs<sup>+</sup>, Ba<sup>2+</sup>, Mg<sup>2+</sup>, Ni<sup>2+</sup>, Pb<sup>2+</sup>, Co<sup>2+</sup>, Ba<sup>2+</sup>, Ag<sup>+</sup>, Cu<sup>2+</sup> (3.0 equiv.) (insert: color change of the TBAs solution after addition of metal ions), UV-vis absorption spectra of (d) **TPA-Br**, (e) **TPA-Py**, (f) **TPA-Py\*** (at  $1.0 \times 10^{-5}$  M in ACN/water solution, 99:1, v/v) with increasing concentrations of Cu<sup>2+</sup> in water (1.0 equiv.) (insert: color change of TBAs solution with increasing concentrations of Cu<sup>2+</sup> from 0 to 1.0 equiv.), EPR spectra of (d) **TPA-Br**, (e) **TPA-Py**, (f) **TPA-Py\*** ( $1.0 \times 10^{-2}$  M in ACN/water solution, 99:1, v/v) in the presence of 1.0 equiv. of Cu<sup>2+</sup>.

Figures 3d-f shows the UV-vis absorption spectra of **TPA-Br**, **TPA-Py** and **TPA-Py\*** upon the addition of increasing concentrations of Cu<sup>2+</sup> in aqueous solution (0-1.0 equiv.). The intensities of the new absorbance peaks in the visible and NIR regions exhibited remarkable increases with a concomitant decrease of the ICT bands (300 nm for **TPA-Br**, 353 nm for **TPA-Py**, 425 nm for **TPA-Py\***) and were accompanied by distinct corresponding color changes (inserts of Figures 3d-f). Additionally, a well-defined isosbestic point clearly appeared in the spectra. The limits of detection (LOD) of **TPA-Br**, **TPA-Py** and **TPA-Py\*** for Cu<sup>2+</sup> were calculated by the formula ( $3\sigma/K$ ) to be  $1.33 \times 10^{-6}$  M,  $5.24 \times 10^{-7}$  M,  $4.95 \times 10^{-7}$  M, respectively (Figure S2), which indicated that the sensitivity of these molecules as colorimetric sensors for Cu<sup>2+</sup> followed the order **TPA-Br** < **TPA-Py** < **TPA-Py\***. The improved sensitivity of the sensors toward the target Cu<sup>2+</sup> cation can be attributed to the increasing ICT effect in the corresponding D-A system. In addition, it seems that no significant interference in the detection of Cu<sup>2+</sup> was observed in the presence of other competitive cations (Figure S3). These results suggested that the TBAs as colorimetric sensors have an excellent selective response for Cu<sup>2+</sup> ions via the formation of radical cations.

Essentially, the new absorption bands formed in the UV and visible regions indicated that the radical cations of the respective aromatic amines formed as a result of an

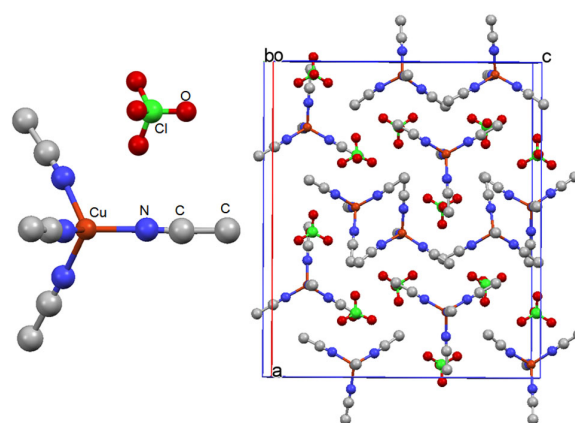


**Figure 4.** X-ray structure of Cu(CH<sub>3</sub>CN)<sub>4</sub>ClO<sub>4</sub> and the packing diagram of the unit cell.

electron transfer reaction between the phenylamine and Cu<sup>2+</sup>.<sup>[10]</sup> In other words, the TPA-based amines are converted to radical cations and Cu<sup>2+</sup> is converted to Cu<sup>+</sup>. In an effort to further confirm the formation of radical cations, electron paramagnetic resonance (EPR) spectra of the

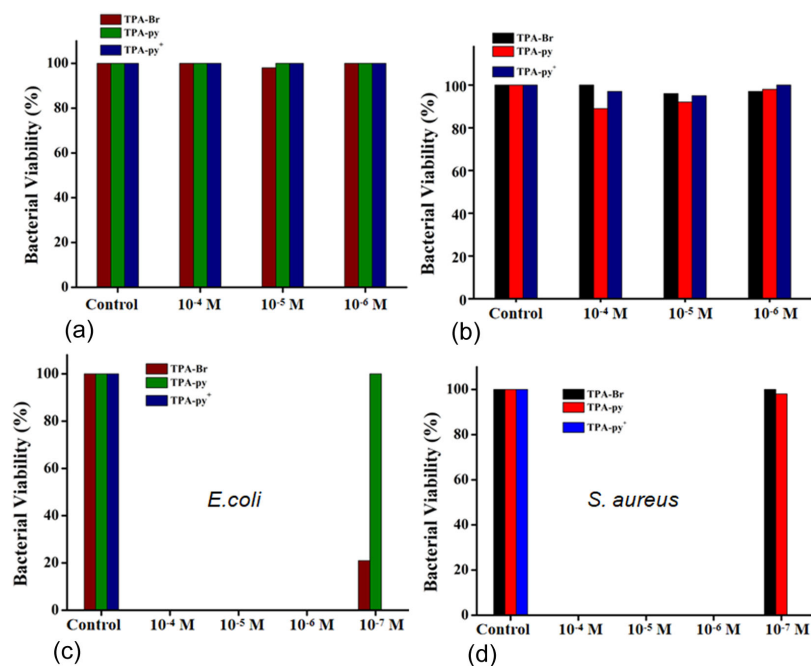


Figure 5. Biocidal activities of TPA-Br, TPA-Py and TPA-Py<sup>+</sup> and the corresponding radical cations at different concentrations toward *E. coli* (a, c) and *S. aureus* interacted (b, d).

solutions were recorded (Figure 3g-i). When 1.0 equiv. of Cu<sup>2+</sup> was added to the ACN solution of the TPA derivatives (TPAs) at room temperature, a similar three-line EPR spectrum in the range of 3490 to 3520 G was observed in all the sample spectra. The *g* value of the radicals was determined to be 2.004, which is similar with the previously reported values of TPA radicals.<sup>[9, 10, 31]</sup> Therefore, this EPR data clearly revealed that radical cations of the TPAs were formed as a result of electron transfer from the parent amine to the Cu<sup>2+</sup>.

Interestingly, the reduction of the Cu<sup>2+</sup> species was successfully observed in the corresponding X-ray structure. Colorless crystals of [Cu(CH<sub>3</sub>CN)<sub>4</sub>][ClO<sub>4</sub>] were obtained by slowly evaporating the mixture solution (ACN/water, 99:1, v/v) of TPA-Br in the presence of 3.0 equiv. of Cu(ClO<sub>4</sub>)<sub>2</sub> at room temperature, which crystallized in the orthogonal system with the Pna21 space group. As shown in Figure 4, the single-crystal X-ray structure of [Cu(CH<sub>3</sub>CN)<sub>4</sub>][ClO<sub>4</sub>] revealed that each copper atom is tetrahedrally coordinated by nitrogen atoms from four almost linear acetonitrile molecules. The acetonitrile molecules are arranged around the copper atoms so that the whole Cu(I) tetra-acetonitrile complex can be described as having an almost ideal tetrahedral symmetry. The corresponding average bond distances in the complex such as Cu–N, N–C, and C–C were found to be 2.01, 1.13, 1.46 Å, respectively. The average Cl–O distance in the perchlorate counter anions was determined to be 1.43 Å. These bond features agree with those found in similar Cu(I) coordination complexes.<sup>[32]</sup> Accordingly, this result further confirmed the reduction of Cu<sup>2+</sup> to Cu<sup>+</sup> in the TPA solutions.

In the past few decades, the emergence of multi-resistant microbial strains due to the abuse of antibiotics poses a serious threat to global public health.<sup>[33]</sup> For example, Gram-negative bacteria can cause severe hospital-acquired infections and are becoming a great threat to most available antibiotic therapies.<sup>[34]</sup> Undoubtedly, it is of great significance to development non-conventional treatments to overcome such a resistance problem. As a result, several strategies including probiotics, antimicrobial peptides, antibodies and bacteriophages have been presented.<sup>[35-37]</sup> Among these approaches, photodynamic therapy, as an efficient deactivation agent (PDI) of microorganisms, has been probed as an alternative methodology to eliminate bacterial diseases in recent years.<sup>[38-40]</sup> In antimicrobial therapy, the PDI agent sensitizes the oxygen in the surroundings to directly or indirectly convert it into reactive oxygen species (ROS) including superoxide anions (O<sub>2</sub><sup>•-</sup>), hydroxyl radicals (HO<sup>•</sup>), and singlet oxygen (<sup>1</sup>O<sub>2</sub>) under light irradiation. Then, the ROS rapidly reacts with proteins or lipids to damage cytoplasmic membranes and this results in the death of microorganisms.<sup>[41,42]</sup> Essentially, the high reactivity of radicals of oxygen is the key factor in the death of the microorganisms. However, because of the instability of most organic radicals in air or aqueous environments, few reports have appeared that directly exploit them as antibacterial agents.

Herein, the TPA derived radical cations were not only stable in ACN solution, but also exhibited good stability in aqueous solutions, even when diluted to 10<sup>-7</sup> M (Figure S4). Thus, it is anticipated that the TPA-based radical cations may be used as antibacterial agents. For this purpose, we investigated the antibacterial activities of the TPAs and their radicals toward *E.*

*coli* and *S. aureus*. These bacteria were chosen as representatives of Gram-negative and Gram-positive strains of great interest because of their ability to produce nosocomial infections. The *E. coli* and *S. aureus* were incubated with **TPAs** and their radical cations in agar plates at different concentrations, respectively, by a traditional surface plating method.<sup>[43]</sup> Photographs of the corresponding agar plates were recorded to observe the growth of *E. coli* and *S. aureus* (Figure 5 and Figure S5). It can be found from Figures 5a,b that the no obvious decrease in the bacterial colony was observed in the presence of the **TPAs**. This result indicated that the two species of microorganisms will not be affected by the neutral **TPA** molecules. However, as shown in Figures 5c,d, the bacterial colony of both microorganisms can be efficiently killed by the corresponding **TPA** radicals at low concentrations. The concentration of **TPA-Br** and **TPA-Py** can be fixed at  $1 \times 10^{-6}$  M, and the lowest concentration of **TPA-Py**<sup>+</sup> can be fixed at  $1 \times 10^{-7}$  M. To further study the antimicrobial mechanism of the **TPA** radicals, the bacterial colony changes of the two species of the representative microorganisms, after incubation with different concentrations of  $\text{Cu}^{2+}$  or  $\text{Cu}^+$  under the same experiment conditions, were performed. Figure S6 shows that *E. coli* and *S. aureus* can survive when the concentrations of  $\text{Cu}^{2+}$  and  $\text{Cu}^+$  are lower than  $1 \times 10^{-5}$  M. Consequently, these results revealed that the **TPA** radical cations play a crucial role in the process of eliminating the bacteria. In the present work, the corresponding radicals can be directly generated by  $\text{Cu}^{2+}$  rather than photo-irradiation. In other words, PDT agents only generate free radicals when exposed to light, which needs a PDT agent,  $\text{O}_2$ , and light,<sup>[38-40]</sup> whereas the direct use of **TPA** radical cations is a more convenient and practical method for killing bacteria.

## Conclusion

In summary, a unique D-A strategy has been exploited to prepare colorimetric sensors for  $\text{Cu}^{2+}$  based on **TPAs**. These sensors exhibited improved sensitivity and selectivity for the detection of  $\text{Cu}^{2+}$  in a mixed solvent of ACN and water via a redox reaction with distinct color changes. In particular, the reduction species of  $\text{Cu(I)}$  from  $\text{Cu(II)}$  was successfully observed in the corresponding X-ray crystal structure. Further studies indicated that the  $\text{Cu}^{2+}$  recognition triggered organic radical cations exhibited good stability in aqueous solutions and have excellent antimicrobial activity against Gram(-) bacteria and Gram(+) bacteria such as *E. coli* and *S. aureus* at relatively low concentration ( $10^{-7}$  M). Importantly, it should be noted that the **TPA**-derived colorimetric sensors and the corresponding organic radicals are easily prepared without complicated functional modification compared to PDT agents. This work thus provides valuable information for the design of sensitive colorimetric sensors for metal ions and potential therapeutic applications of organic radicals for pathogenic infections caused by drug-resistant bacteria.

## Supporting Information Summary

Experimental section, UV-vis absorption spectra of  $\text{Cu(ClO)}_2$ , limit of detection, interference experiment in the detection of  $\text{Cu}^{2+}$ , stability experiment of the corresponding radicals in water,

plate images showing the the growth of *E. coli* and *S. aureus* in the presence and absence of radicals,  $\text{Cu}^{2+}$  and  $\text{Cu}^+$ .

## Acknowledgements

We acknowledge the support of National Natural Science Foundation of China (No. 21871063). CR thanks the EPSRC for the award of an Overseas Travel Grant (EP/R023816/1).

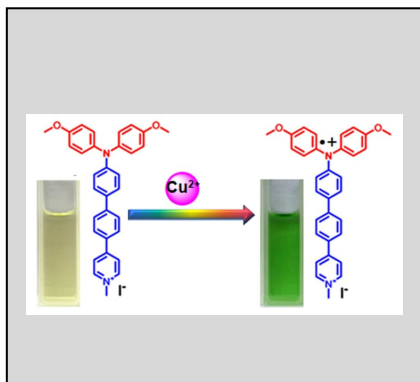
**Keywords:** antibacterial agent • chemosensor • copper ion • radical • triphenylamine

- [1] Y. Rajca, M. Wang, J. T. Boska, A. Paletta, M. A. Olankitwanit, D. G. Swanson, S. S. Mitchell, G. R. Eaton, S. Rajca, *J. Am. Chem. Soc.* **2012**, *134*, 15724–15727.
- [2] H. Garcia, H. D. Roth, *Chem. Rev.* **2002**, *102*, 3947–4008.
- [3] K. Zhang, M. J. Monteiro, Z. Jia, *Poly. Chem.* **2016**, *7*, 5589–5614.
- [4] M. Mas-Torrent, N. Crivillers, C. Rovira, J. Veciana, *Chem. Rev.* **2012**, *112*, 2506–2527.
- [5] N. G. Connelly, W. E. Geiger, *Chem. Rev.* **1996**, *96*, 877–910.
- [6] M. R. Ajayakumar, D. Asthana, P. Mukhopadhyay, *Org. Lett.* **2012**, *14*, 4822–4825.
- [7] K. Nie, B. Dong, H. Shi, L. Chao, X. Duan, X.-F. Jiang, Z. Liu, B. Liang, *Dyes Pigm.* **2019**, *160*, 814–822.
- [8] X. Zhang, M. Kang, H.-A. Choi, J. Y. Jung, K. M. K. Swamy, S. Kim, D. Kim, J. Kim, C. Lee, J. Yoon, *Sens. Actuators, B* **2014**, *192*, 691–696.
- [9] K. Sreenath, T. G. Thomas, K. R. Gopidas, *Org. Lett.* **2011**, *13*, 1134–1137.
- [10] S. Sumalekshmy, K.R. Gopidas, *Chem. Phys. Lett.* **2005**, *413*, 294–299.
- [11] X. Wu, Z. Guo, Y. Wu, S. Zhu, T. D. James, W. Zhu, *ACS Appl. Mater. Interfaces* **2013**, *5*, 12215–12220.
- [12] T. G. Thomas, K. Sreenath, K. R. Gopidas, *Analyst*, **2012**, *137*, 5358–5362.
- [13] G. Sathiyam, S. Chatterjee, P. Sen, A. Garg, R. K. Gupta, *ChemistrySelect* **2019**, *4*, 11718–11725.
- [14] X. Nan, Y. Huyan, H. Li, S. Sun, Y. Xu, *Coord. Chem. Rev.* **2021**, *426*, 213580.
- [15] L. Tapia, M. Suazo, C. Hodar, V. Cambiazo, M. Gonzalez, *BioMetals* **2003**, *16*, 169–174.
- [16] D. J. Waggoner, T. B. Bartnikas, J. D. Gitlin, *Neurobiol. Dis.* **1999**, *6*, 221–230.
- [17] D. Strausak, J. F. Mercer, H. H. Dieter, W. Stremmel, G. Multhaup, *Brain Res. Bull.* **2001**, *55*, 175–185.
- [18] E. Gaggelli, H. Kozlowski, D. Valensin, G. Valensin, *Chem. Rev.* **2006**, *37*, 1995–2044.
- [19] G. Sivaraman, M. Iniya, T. Anand, N. G. Kotla, O. Sunnapu, S. Singaravadivel, A. Gulyani, D. Chellappa, *Coord. Chem. Rev.* **2018**, *357*, 50–104.
- [20] D. Cao, Z. Liu, P. Verwilt, S. Koo, P. Jangjili, J. S. Kim, W. Lin, *Chem. Rev.* **2019**, *119*, 10403–10519.
- [21] J. A. Cotruvo, Jr., A. T. Aron, K. M. Ramos-Torres, C. J. Chang, *Chem. Soc. Rev.* **2015**, *44*, 4400–4414.
- [22] D. S. McClure, *J. Chem. Phys.* **1952**, *20*, 682–686.
- [23] D. Udhayakumari, S. Nahaa, S. Velmathi, *Anal. Methods* **2017**, *9*, 552–578.
- [24] Z. Kowser, U. Rayhan, T. Akther, C. Redshaw, T. Yamato, *Mater. Chem. Front.* **2021**, *5*, 2173–2200.
- [25] G. MartinsFernandes, W. R.Silva, D. NunesBarreto, R. S. Lamarca, P. C. F. L. Gomes, S. Petrucci, A. D. Batista, *Anal. Chim. Acta.* **2020**, *1135*, 187–203.
- [26] H. N. Abdelhamid, H.-F. Wu, *RSC Adv.* **2015**, *5*, 50494–50504.
- [27] M. Scarongella, A. Laktionov, U. Rothlisberger, N. Banerji, *J. Mater. Chem. C* **2013**, *1*, 2308–2319.
- [28] J. Roncali, *Chem. Rev.* **1992**, *92*, 711–738.
- [29] K. Takimiya, I. Osaka, M. Nakano, *Chem. Mater.* **2014**, *26*, 587–593.

- 
- [30] J. Wang, X. Li, J. Zhang, H. Tian, *Sens. Actuators, B* **2018**, *257*, 77–86.
- [31] C. Hassenrück, R. F. Winter, *Inorg. Chem.* **2017**, *56*, 13517–13529.
- [32] I. Csöreg, P. Kierkegaard, R. Norrestam, *Acta Cryst. B* **1975**, *31*, 314–317.
- [33] Y. H. Niu, R. E. Wang, H. F. Wu, J. F. Cai, *Future Med. Chem.* **2012**, *4*, 1853–1862.
- [34] X. Z. Li, P. Plesiat, H. Nikaido, *Clin. Microbiol. Rev.* **2015**, *28*, 337–418.
- [35] C. Ghosh, P. Sarkar, R. Issa, J. Haldar, *Trends Microbiol.* **2019**, *27*, 323–338.
- [36] H. N. Abdelhamid, M. S. Khane, H.-F. Wu, *RSC Adv.* **2014**, *4*, 50035–50046.
- [37] B.-S. Wu, H. N. Abdelhamid, H.-F. Wu, *RSC Adv.* **2014**, *4*, 3722–3731.
- [38] D. van Straten, V. Mashayekhi, H. S. de Bruijn, S. Oliveira, D. J. Robinson, *Cancers* **2017**, *9*, No. 19.
- [39] T. Dai, Y. Y. Huang, M. R. Hamblin, *Photo. Photodyn. Ther.* **2009**, *6*, 170–188.
- [40] H. Chen, S. Li, Wu, M.; Z. Huang, C.-S. Lee, B. Liu, *Angew. Chem., Int. Ed.* **2020**, *59*, 632–636.
- [41] A. Almeida, M. A. F. Faustino, J. P. C. Tome, *Future Med. Chem.* **2015**, *7*, 1221–1224.
- [42] M. R. Hamblin, T. Hasan, *Photochem. Photobiol. Sci.* **2004**, *3*, 436–450.
- [43] H. Yuan, H. Chong, B. Wang, C. L. Zhu, L. B. Liu, Q. Yang, F. T. Lv, S. Wang, *J. Am. Chem. Soc.* **2012**, *134*, 13184–13187.

---

## Entry for the Table of Contents



A novel organic radical cation-based colorimetric sensor for  $\text{Cu}^{2+}$  was reported, in particular, the reduction species of Cu (I) from Cu (II) was successfully observed in the corresponding X-ray structure. Further study revealed that the  $\text{Cu}^{2+}$  recognition triggered organic radical cations shows excellent antibacterial efficiency.